



## Brain tumor classification with convolutional neural network

---

Mohamed Shoaib, Mohamed Elshamy, Taha Taha,  
Adel El-Fishawy and Fathi Abd El-Samie

EasyChair preprints are intended for rapid dissemination of research results and are integrated with the rest of EasyChair.

July 3, 2021

# Brain tumor classification with convolutional neural network

Mohamed R. Shoaib<sup>1</sup>, Mohamed R. Elshamy<sup>2</sup>, Taha E. Taha<sup>3</sup>, Adel S. El-Fishawy<sup>4</sup>, Fathi E. Abd El-Samie<sup>5</sup>

<sup>1</sup>Faculty of electronic engineering, Menoufia university, Egypt  
E-mail: mohammed\_reda1996@outlook.com

<sup>2</sup> Faculty of electronic engineering, Menoufia university, Egypt  
E-mail: [moh.elshamy@el-eng.menofia.edu.eg](mailto:moh.elshamy@el-eng.menofia.edu.eg)

<sup>3</sup> Faculty of electronic engineering, Menoufia university, Egypt  
E-mail: taha117@hotmail.com

<sup>4</sup> Faculty of electronic engineering, Menoufia university, Egypt  
E-mail: aelfshawy@hotmail.com

<sup>5</sup> Faculty of electronic engineering, Menoufia university, Egypt  
E-mail: fathi\_sayed@el-eng.menofia.edu.eg

**Abstract.** Brain tumor is an acute cancerous disease that results from abnormal and uncontrollable cell division. Brain tumors are classified by biopsy, which is not usually performed before final surgery of the brain. Recent advances and improvements in technology in deep learning have helped the health industry in medical imaging for the medical diagnosis of many diseases. A deep learning algorithm that has yielded substantial results in image segmentation and classification is the Convolutional Neural Network (CNN). Similarly, in our paper, we introduce the convolutional neural network (CNN) approach along with Image Processing to categorize brain MRI scan images into four classes which are glioma tumor, meningioma tumor, pituitary tumor and normal patients. Using the transfer learning approach and a CNN based model from scratch we compared the performance of our scratched CNN model with pre-trained inceptionresnetv2, inceptionv3 models. The experiment is tested on a brain tumor MRI dataset which contains (826) MRI images for glioma tumor patients, (822) MRI images for meningioma tumor patients, (827) MRI images for pituitary tumor patients and (835) MRI images for normal persons. but the experimental result shows that our model accuracy result is very effective and have very low complexity rate by achieving 93.15% accuracy for the transfer learning model, while inceptionresnetv2 achieved 86.80%, inceptionv3 achieved 85.34% and BRAIN-TUMOR-net based CNN achieved 91.24% accuracy. Our model requires very less computational power and has much better accuracy results as compared to other pre-trained models.

## 1. Introduction

Brain tumor means the proliferation of abnormal cells in brain tissue [7]. It is a collection, or mass, of

---

<sup>2</sup> Mohamed R. Elshamy

abnormal cells in your brain. Your skull, which encloses your brain, is very rigid. Any growth inside such a restricted space can cause problems. Brain tumors can be cancerous (malignant) or noncancerous (benign). Brain tumors are categorized as primary or secondary. A primary brain tumor originates in your brain. Many primary brain tumors are benign. A secondary brain tumor, also called a metastatic brain tumor, take place when cancer cells spread to your brain from another organ, such as your lung or breast.

A primary brain or spinal cord tumor is a tumor that occurs at first in the brain or spinal cord. This year, an estimated 24,530 adults (13,840 men and 10,690 women) in the United States have been diagnosed with primary cancerous tumors of the brain and spinal cord. The likelihood of a person developing this type of tumor in their lifetime is less than 1%. Brain tumors represent for 85% to 90% of all primary central nervous system (CNS) tumors. About 3,460 children under the age of 15 will be diagnosed with a brain or central nervous system tumor this year. The remainder of this guide deals with primary brain tumors in adults. Common brain tumor infection Symptoms and Signs include [9]: Headaches, Seizures, Personality or memory changes, Nausea or vomiting, Fatigue, Drowsiness, Sleep problems, Memory problems, and Changes in ability to walk or perform daily activities. Symptoms that may be specific to the tumor site contains of pressure or headache near the tumor, loss of balance and difficulty with fine motor skills. Vision changes, including loss of part of the vision or double vision, and Inability to look upward can be caused by a pineal gland tumor.

Several studies comparing CT and MRI for brain evaluation have shown MRI to be more sensitive, although not more specific [10]. The advantages of MRI center on its ability to reveal abnormalities that may not be detectable or only poorly seen on CT. In situations where only a nonspecific group effect can be visualized on CT scans, the MRI may determine the exact scope and location of the tumor. Moreover, MRI with increased contrast discrimination and its ability to obtain images at many levels can better determine the precise location of the lesion in relation to major neuroanatomical structures. So, we use the MIR data set in this study with different deep learning models for making a comparison study.

This paper presents a deep learning (DL) model for automatic brain tumor diagnosis. Different learning strategies is studied for early brain tumor detection. The first and the second strategies depend on the utilization of pre-trained models such, the inceptionresnetv2 and inceptionv3. Also, a transfer-based learning is introduced. In addition to, a CNN that is called, BRAINTUMOR-net trained from scratch for brain tumor detection. The proposed models are evaluated on MRI brain tumor [16] dataset. A comparison between the proposed model and other state-of-art methods is introduced.

## 2. Related work

There are many machine learning and deep learning systems that has been suggested for brain tumor detection from MRI and CT images. Several studies corroborate the efficiency of MRI and employ image processing tools to detect brain tumor. MRI scanners are utilized to generate images of the organs in the body like what is done with fractures, bone dislocations, lung infections, pneumonia, and COVID-19. Many researchers provided machine learning, deep learning, and image processing-based methods for brain tumor detection.

Fuyong Xing, Yuanpu Xie, Lin Yang [1] presented The HySIME algorithm initial filtering by deep CNN followed by iterative region merging segmentation by selective sparse shape model. It has advantages of Reduction of computing time, suitable for real time applications. The proposed algorithm achieved 85% and Sensitivity of 89%. HT. Zaw, N. Maneerat, KY. Win. [2] Used Morphological operation, pixel subtraction, and Maximum entropy threshold segmentation to make a Segmentation Preprocessing for improving the diagnostic performance of the human-machine combination using available brain tumor MRI dataset.

However, this paper used the Morphological, Intensity as features with Naive Bayes classifier and achieved only an accuracy of 94 %.

TL. Narayana, TS. Reddy [3] presented a Median filter GA segmentation algorithm for segmentation process. However, this paper used the GLCM as features with SVM classifier for Harvard Medical Dataset and achieved only an accuracy of 91.23%. A. Minz, C. Mahobiya. [4] used the Median filter noise removal; Threshold based segmentation to image segmentation for improving the diagnostic performance of the human-machine combination using available public brain tumor MRI dataset. However, this paper achieved only an accuracy of 89.90 %.

Astina Minz, Prof. Chandrakant Mahobiya (2017) 89. [5] presented an algorithm for brain tumor detection; where in this paper this algorithm minimizes the error, less time consuming but it has limitation of It can maximize the margin with respect to features that have already been selected. Their algorithm reported an accuracy of 89.90% & 74.00%. AR. Raju, P. Suresh, RR. Rao, [6].in this paper the Bays scan fuzzy clustering segmentation, information theoretic scatters and wavelet features are used for pre-processing for COVID-19 detection. Bayesian HCS-based multi-SVNN classifier is used for brain tumor detection. They reported 93% for accuracy.

### 3. Materials and Methods

#### 3.1 Datasets

The proposed machine learning framework is tested on the dataset of MRI brain tumor. The MRI brain tumor dataset [16] contains (826) MRI images for glioma tumor patients, (822) MRI images for meningioma tumor patients, (827) MRI images for pituitary tumor patients and (835) MRI images for normal patients. Figure (2) presents different samples for glioma tumor, meningioma tumor patients, pituitary tumor patients and normal persons from the dataset that used to examine the model.

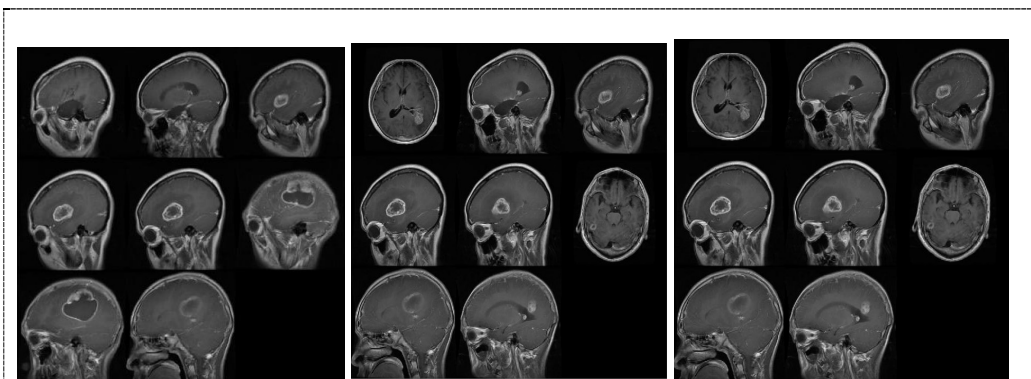
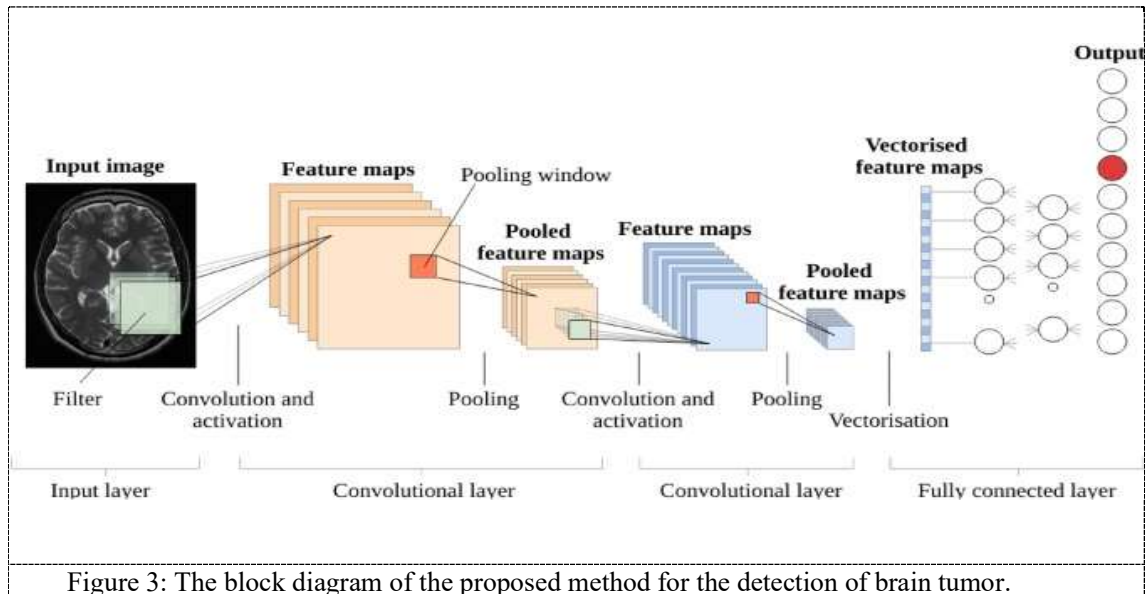


Figure 2: presents different samples for glioma tumor, meningioma tumor patients, pituitary tumor patients and normal persons from the dataset that used to examine the model

#### 3.2 Classification of MRI image.

Deep learning models have been used in many areas such as classification, segmentation and lesion detection of medical data. The medical image obtained from medical imaging techniques such as magnetic resonance imaging, X-ray images and CT images. (MRI), computed tomography (CT) and X-ray can be analyzed with the help of machine learning models [20–24] and deep learning models. In this paper, different deep learning models for diagnosing tumor patients based on classifying MRI images to normal, glioma tumor, meningioma tumor or pituitary tumor classes is introduced. The block diagram of the proposed method for the detection of brain tumor is presented in Fig 3.



Generally, a CNN model consists of many layers which are [23, 24, 25, 26 and 27]: input layer, convolutional layers, pooling layers, full-connection layers, and output layer. The proposed BRAIN-TUMOR-net CNN model has the following architecture:

- Input layer: The inputs are MRI images with image dimension of  $244 \times 244$ .
- COVN layers: It consists of three layers, convolutional layer (Conv), BN layer and Relu layer. Convolutional layer is used to capture the features of the entire image and compress it into feature maps. Thus, we perform three convolutions over the input images using multiple filters (8, 16, 32, 64 and 128) for the first, second, third, fourth and fifth Conv, respectively with fixed widow size of 3. Batch normalization layers are used for optimizations in order to reduce the overfitting and obtain better test accuracy. Where the activations of the previous layer for each batch during training is normalized. Relu activation functions are used to incorporate element-wise non-linearity.
- Pooling layer: It is used to extract the most applicable features within each feature map. We use the max-pooling strategy for the pooling operation. All vectors that are

obtained from the max-pooling layer are used to obtain a fixed-length feature vector. The max pooling is set to  $2 \times 2$  with a stride of 2.

- Fully connected layers (FC): Treats the input data as a simple vector and produce an output as a single vector. We have 4 FC layer in the proposed model. The last one, a fully connected output layer with SoftMax activation for classifying the input images into four classes.

### 3.3 Performance Metrics.

The confusion matrix has quadrant expected outcomes as follows: true positive (Tp) is the number of correctly diagnosed anomalous cases. True negative (Tn) is the number of correctly identified normal cases. False positive (Fp) is a set of normal cases which are classified as anomaly diagnoses. False negative (Fn) is a set of anomalies observed as normal. The overall performance analysis for each deep learning classifier will be evaluated based on sensitivity (Sen), specificity (Spec), accuracy (Acc), precision (Preci), Matthew's correlation coefficient (MCC), false positive rate (FPR), error, Kappa and F1\_score.

**Table 1.** confusion matrix

	Actually positive (1)	Actually negative (0)
Predicted positive	True positive (TPS)	False positive (FPS)
Predictive negative	False negative (FNS)	True negative (TNS)

The confusion matrix has four predicted outcomes as follows: True positive ( $Tp$ ) is the number of anomalies that are correctly diagnosed. Negative true ( $Tn$ ) is the number of correctly identified normal states. False positive ( $Fp$ ) is A group of normal conditions that are classified as abnormal diagnoses. False Negative ( $Fn$ ) is a group of anomalies normally observed [13].

This is a list of rates that are often computed from a confusion matrix for a binary classifier:

Accuracy: Overall, how often is the classifier correct.

$$ACC = (Tp + Tn) / ((Tp + Tn) + (Fp + Fn)) * 100 \quad (1)$$

False Positive Rate: When it's actually no, how often does it predict yes.also known as "Sensitivity" or "Recall"

$$FPR = FP / (Fp + Tn) \quad (2)$$

True Positive Rate: When it's actually yes, how often does it predict yes.

$$Sen = TP/(Fn + Tp) \quad (3)$$

True Negative Rate: When it is actually no, how often does it predict no. equivalent to 1 minus False Positive Rate also known as "Specificity"

$$Spec = TN/(Fp + Tn) \quad (4)$$

Precision: When it predicts yes, how often is it correct.

$$Preci = TP/(Fp + Tp) \quad (5)$$

Prevalence: How often does the yes condition actually occur in our sample.

$$Prev = (Fn + Tp)/((Tp + Tn) + (Fp + Fn)) \quad (6)$$

The Matthews correlation coefficient (MCC), invented by Brian Matthews in 1975, is a tool for model evaluation. It measures the differences between actual values and predicted values and is equivalent to the chi-square statistic for a 2 x 2 contingency table (Kaden et al., 2014) [12].

$$MCC = \frac{T_N * T_P - F_N * F_b}{\sqrt{(T_P + F_b)(T_P + F_N)(T_N + F_b)(T_N + F_N)}} \quad (7)$$

The F-score or F-measure is a measure of a test's accuracy. It is calculated from the precision and recall of the test, where the precision is the number of true positive results divided by the number of all positive results, including those not identified correctly, and the recall is the number of true positive results divided by the number of all samples that should have been identified as positive. The F1 score is the harmonic mean of the precision and recall [14].

$$F1 \text{ score} = 2 * (Precision \cdot Recall / (Precision + Recall)) \quad (8)$$

Kappa Statistic compares the accuracy of the system to the accuracy of a random system. To quote Richard Landis and Gary Koch from the 1977 paper The Measurement of Observer Agreement for Categorical Data, “. (Total accuracy) is an observational probability of agreement and (random accuracy) is a hypothetical expected probability of agreement under an appropriate set of baseline constraints.” [17].

$$k = \frac{P_o - P_e}{1 - P_e} \quad (9)$$

Where  $P_o$  is the overall accuracy of the model and  $P_e$  is the measure of the agreement between the model predictions and the actual class values as if happening by chance.[15]

#### 4. Result and discussion

In this paper, four different deep learning models have been used for the detection of brain tumor disease patients. Popular pretrained deep learning models such as inceptionresnetv2, inceptionv3 have been trained and tested on MRI images. Also, a transfer learning model based on CNN pretrained model and a deep CNN model from scratch have been used for brain tumor detection with the same MRI image dataset.

Table 2 Detection performance results obtained from different deep learning models for 75/25 train and testing ratio performed on the dataset.

Models	Evaluation metric								
	ACC	SEN	SPE	Preci	F1_score	MCC	Error	Kappa	FPR
inceptionresnetv2	0.8680	0.8680	0.9560	0.8685	0.8683	0.8242	0.1320	0.6480	0.0440
inceptionv3	0.8534	0.8534	0.9511	0.8512	0.8498	0.8036	0.1466	0.6091	0.0489
transfer learning model	0.9315	0.9314	0.9772	0.9314	0.9311	0.9085	0.0685	0.8174	0.0228
BRAIN-TUMOR-net	0.9124	0.9122	0.9708	0.9120	0.9108	0.8829	0.0876	0.7664	0.0292

##### 4.1 Results for The First pretrained model (inceptionresnetv2)

For the first pretrained model [18] with 75/25 train and test ratio for MRI image dataset reported the performance metric which are 0.8680, 0.8680, 0.9560, 0.8685, 0.8683, 0.8242, 0.1320, 0.6480, 0.0440 for Accuracy, Sensitivity, Specificity, Precision, F1\_score, Matthews Correlation Coefficient, Error, Kappa and False Positive Rate, respectively. Figure 4 presents the confusion matrix and ROC curve of brain tumor types and normal which are glioma tumor, meningioma tumor and pituitary tumor test results which are trained and tested using inceptionresnetv2 pretrained model. The model achieved a 90% area under curve (AUC). Detection performance results with 75/25 train and test ratio for inceptionresnetv2 pretrained learning model are presented in Table 2.



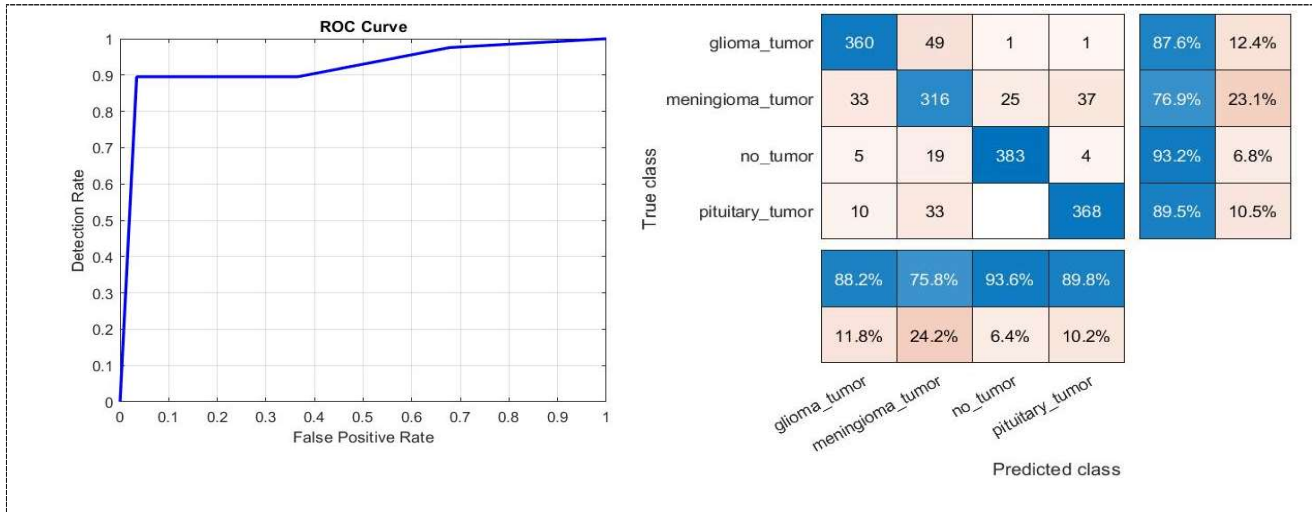


Figure 4: presents the confusion matrix and ROC curve of brain tumor types for the inceptionresnetv2 .

#### 4.2 Result for the second pretrained model (inceptionv3)

For the first pretrained model [19] also use the same train and test ratio which are 75/25 respectively for the same MRI image dataset reported the performance metric which are 0.8534, 0.8534, 0.9511, 0.8512, 0.8498, 0.8036, 0.1466, 0.6091, 0.0489 for Accuracy, Sensitivity, Specificity, Precision, F1\_score, Matthews Correlation Coefficient, Error, Kappa and False Positive Rate respectively. Figure 5 presents the confusion matrix and ROC curve of brain tumor types and normal which are glioma tumor, meningioma tumor and pituitary tumor test results which are trained and tested using inceptionv3 pretrained model. The model achieved a 95% area under curve (AUC). Detection performance results with 75/25 train and test ratio for inceptionv3 pretrained learning model are presented in Table 2.

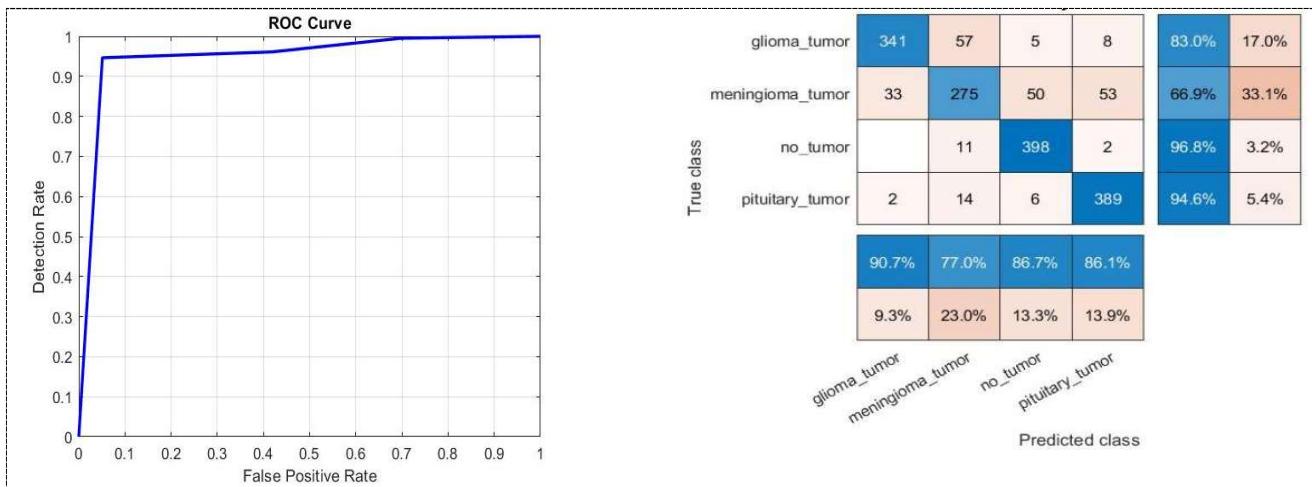


Figure 5: presents the confusion matrix and ROC curve of brain tumor types for the inceptionv3.

### 4.3 Result for the Third CNN Model (Transfer Learning Model)

Figures 6 and 7 present confusion matrices and ROC curves by using the transfer learning model based on CNN [17] and the training progress curve respectively this classifiers give higher performance than other models for the same dataset where it contains (826) MRI images for glioma tumor patients, (822) MRI images for meningioma tumor patients, (827) MRI images for pituitary tumor patients and (835) MRI images for normal persons. The model has achieved the following performance metric, which is 0.9315, 0.9314, 0.9772, 0.9314, 0.9311, 0.9085, 0.0685, 0.8174, and 0.0228 for Accuracy, Sensitivity, Specificity, Precision, F1\_score, Matthews Correlation Coefficient, Error, Kappa and False Positive Rate, respectively. The Transfer Learning Model based on CNN is the best model for brain tumor detection and classification. Figure 6 presents the confusion matrix and ROC curve of brain tumor types and normal which are glioma tumor, meningioma tumor and pituitary tumor test results which are trained and tested using Transfer Learning Model. The model achieved a 98% area under curve (AUC). Also figure 7 presents the training progress of the transfer learning model and it achieved a validation accuracy of 100%. Detection performance results with 75/25 train and test ratio for the transfer learning model are presented in Table 2.

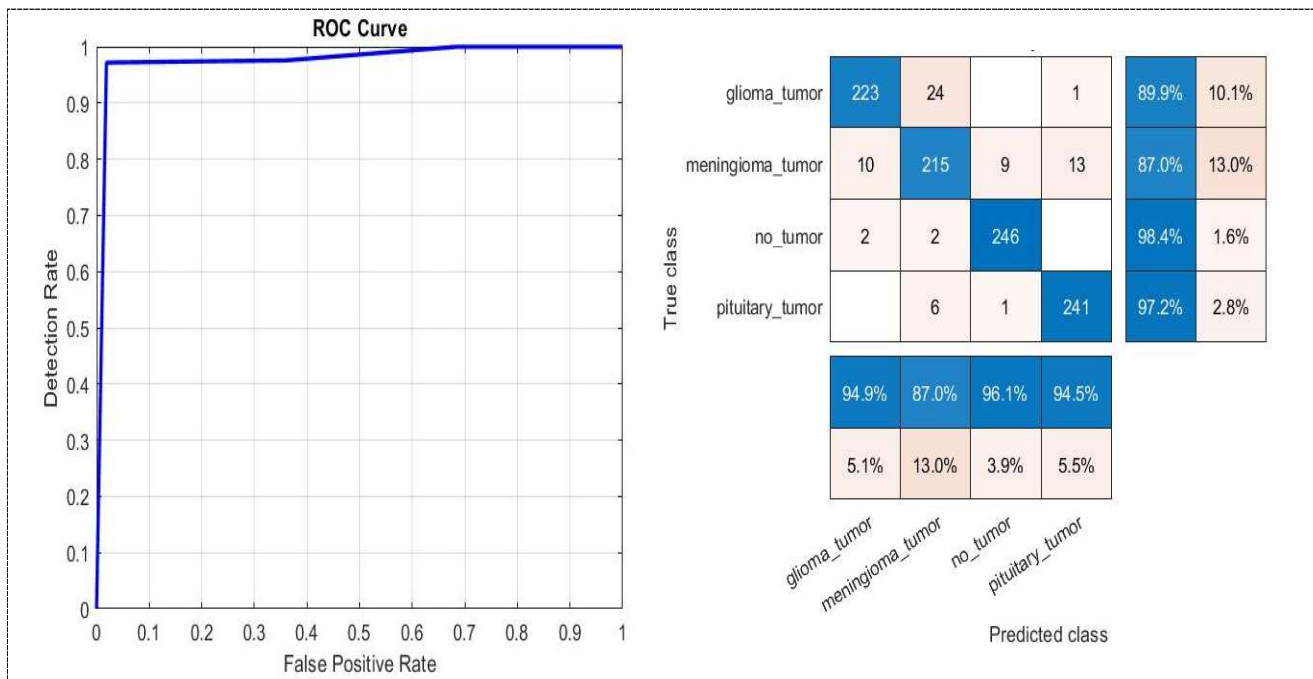


Figure 6: presents the confusion matrix and ROC curve of brain tumor types for the transfer learning.

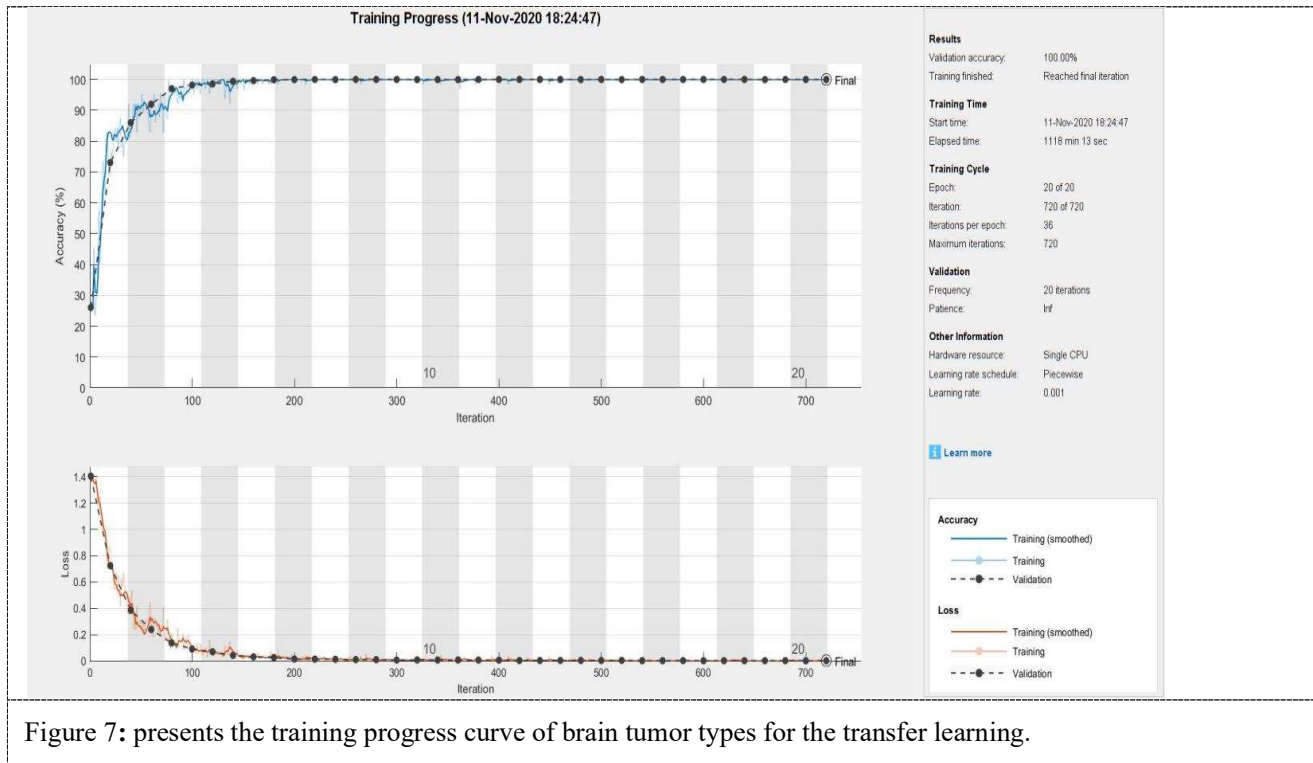


Figure 7: presents the training progress curve of brain tumor types for the transfer learning.

#### 4.4 Result for the Fourth CNN Model (BRAIN-TUMOR-net Model)

Confusion matrices, ROC and training progress curves of brain tumor types and normal which are glioma tumor, meningioma tumor and pituitary tumor test results by using the brain tumor dataset [18] are presented in figures 8 and 9 respectively. The BRAIN-TUMOR-net model has achieved the following performance metric, which is 0.9315, 0.9314, 0.9772, 0.9314, 0.9311, 0.9085, 0.0685, 0.8174, and 0.0228 for Accuracy, Sensitivity, Specificity, Precision, F1\_score, Matthews Correlation Coefficient, Error, Kappa and False Positive Rate respectively. The model achieved a 98% area under curve (AUC). Also figure 9 presents the training progress of the transfer learning model and it achieved a validation accuracy of 100%. Detection performance results with 75/25 train and test ratio for the transfer learning model are presented in Table 2.

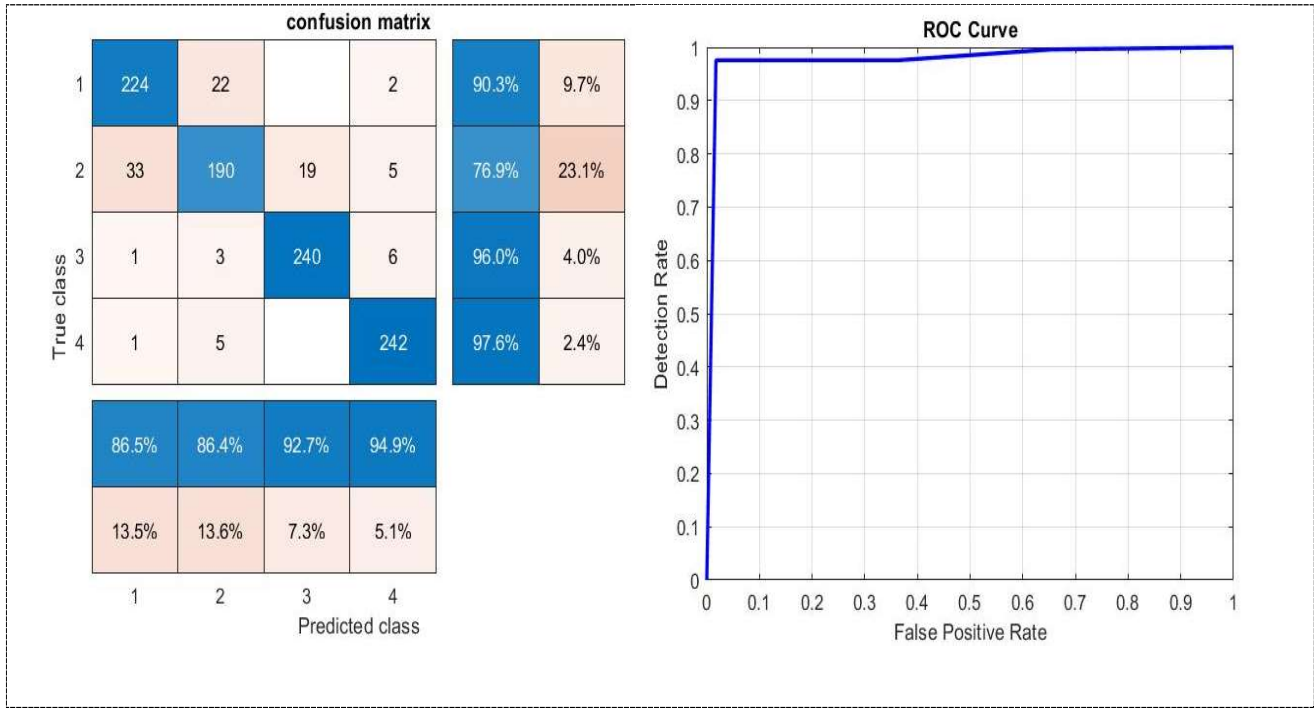


Figure 8 :presents the confusion matrix and ROC curve of brain tumor types for the BRAIN-TUMOR-net Model.

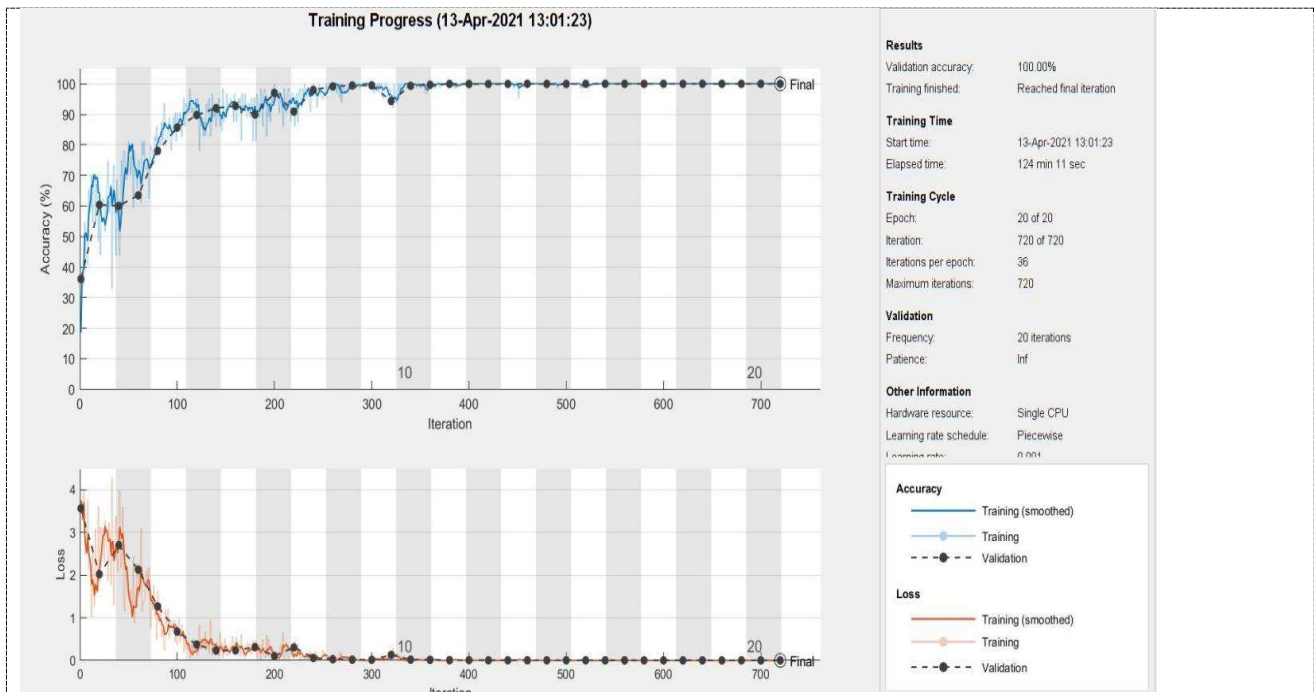


Figure 9 :presents the training progress curve of brain tumor types for the BRAIN-TUMOR-net Model.

#### 4.5 Practical implementation for brain tumor detection

In this section an experiment for showing the result of the proposed machine learning models in real time to make it easier for those who will use the model so that they can see the results of the model from anywhere or from network. After running the model, the model was trained on the training dataset then the model was tested using the test dataset and the output is connected to a hardware circuit via serial port to show the output of the model on LCD screen as shown in Fig. 10.

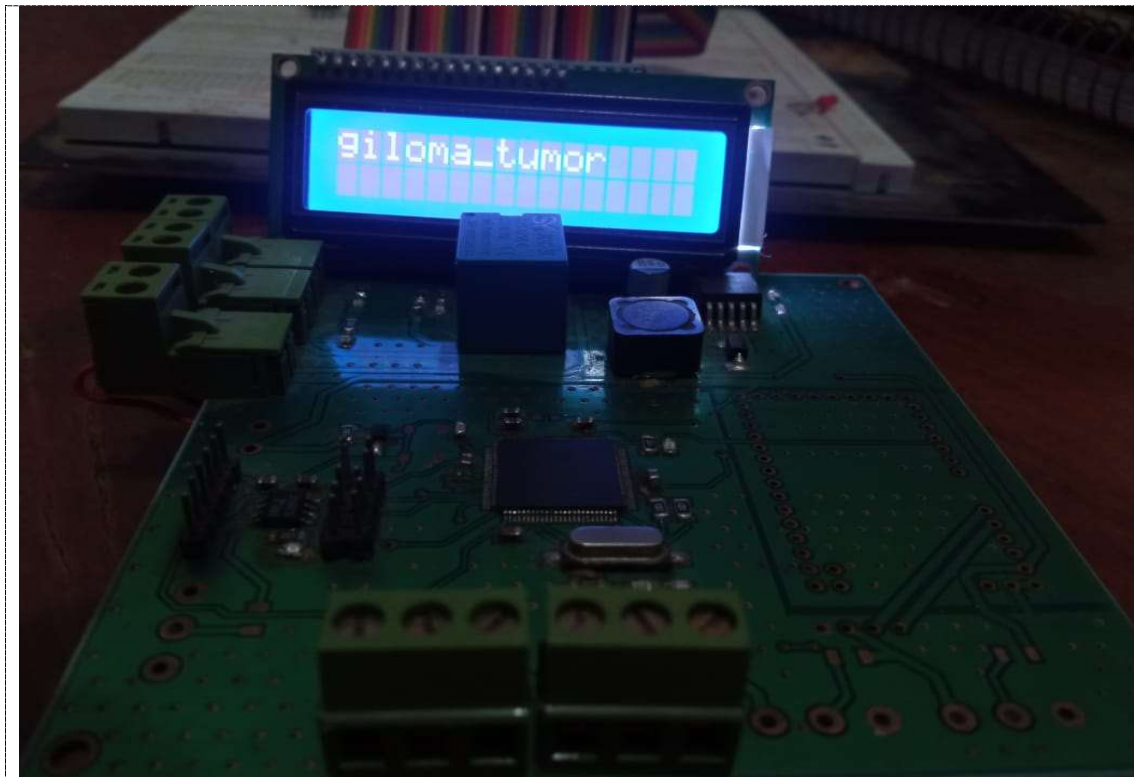


Figure 10 :presents the Practical implementation for brain tumor detection

#### 5. Conclusion

A comparison study between four CNN architecture-based models for brain tumor classification was presented in this study. The classification was performed using a brain tumor MRI image database which contains four classes three of them are brain tumor types and the remaining category is the normal class. also, it was not necessary to perform any preprocessing or segmentation of the tumors because of the benefits of using CNN model based which requires many less resources for both training and implementation. A comparison with the comparable state-of-the-art methods shows that the transfer learning model-based CNN obtained better

results. This model achieved 93.15%, 93.14%, 97.72%, 93.14%, 93.11%, 90.85%, 0.0685, 81.74%, and 0.0228 for Accuracy, Sensitivity, Specificity, Precision, F1\_score, Matthews Correlation Coefficient, Error, Kappa and False Positive Rate respectively. For further work, we will look at other approaches to expanding the database (For example, increasing the number of topics) in order to improve the scalability of the network. One of the major improvements would be to modify the structure of the deep learning model so that it can be used during the brain Surgery, tumor classification and precise location. Detection of tumors in the operating room It must be implemented in real time and in real-world conditions; Hence, in this case, the improvement It also includes adapting the grid to a 3D system. By keeping the network architecture simple, Real-time detection may be possible. In the future, we will check our design performance The neural network, as well as the improved one, on other medical images.

## 6. References

- [1] Fuyong Xing, Yuanpu Xie, Lin Yang, "An Automatic LearningBased Framework for Robust Nucleus Segmentation", IEEE TRANSACTIONS ON MEDICAL IMAGING, VOL. 35, NO. 2, pp- 550-566, 2016
- [2] HT. Zaw, N. Maneerat, KY. Win, —Brain tumor detection based on Naïve Bayes classification, International Conference on Engineering, Applied Sciences and Technology, pp.1-4, 2019
- [3] TL. Narayana , TS.Reddy, An Efficient Optimization Technique to Detect Brain Tumor from MRI Images, International Conference on Smart Systems and Inventive Technology, pp.1-4, 2018
- [4] A.Minz , C. Mahobiya , MR Image classification using adaboost for brain tumor type, IEEE 7th International Advance Computing Conference, pp.1-5, 2017
- [5] Astina Minz, Prof. Chandrakant Mahobiya "MR Image classification using Adaboost for brain tumor type" in IEEE 7th International Advance Computing Conference (IACC) 2017
- [6] AR.Raju , P.Suresh , RR.Rao, Bayesian HCS-based multi-SVNN: A classification approach for brain tumor segmentation and classification using Bayesian fuzzy clustering, Biocybernetics and Biomedical Engineering, pp.646-660, 2018
- [7] <https://www.healthline.com/health/brain-tumor>
- [8] <https://www.cancer.net/cancer-types/brain-tumor/statistics>
- [9] <https://www.cancer.net/cancer-types/brain-tumor/symptoms-and-signs>
- [10] Maravilla KR, Sory WC. Magnetic resonance imaging of brain tumors. Semin Neurol. 1986 Mar;6(1):33-42. doi: 10.1055/s-2008-1041445. PMID: 3332409.
- [11] <https://acsjournals.onlinelibrary.wiley.com/doi/full/10.3322/caac.21660>
- [12] Kaden, M. et al., (2014). Optimization of General Statistical Accuracy Measures for Classification Based on Learning Vector Quantization. ESANN 2014 proceedings, European Symposium on Artificial Neural Networks, Computational Intelligence
- [13] <https://www.dataschool.io/simple-guide-to-confusion-matrix-terminology>
- [14] Sasaki, Y. (2007). "The truth of the F-measure". <https://www.toyota-ti.ac.jp/Lab/Denshi/COIN/people/yutaka.sasaki/F-measure-YS-26Oct07>
- [15] <https://thenewstack.io/cohens-kappa-what-it-is-when-to-use-it-and-how-to-avoid-its-pitfalls/>
- [16] <https://www.kaggle.com/sartajbhuvaji/brain-tumor-classification-mri>
- [17] <https://www.standardwisdom.com/2011/12/29/confusion-matrix-another-single-value-metric-kappa-statistic/>

- [18] Szegedy, Christian, Sergey Ioffe, Vincent Vanhoucke, and Alexander A. Alemi. "Inception-v4, Inception-ResNet and the Impact of Residual Connections on Learning." In AAAI, vol. 4, p. 12. 2017.
- [19] <https://www.apriorit.com/dev-blog/606-inception-v3-for-video-classification>
- [20] O. Yildirim, M. Talo, B. Ay, U. B. Baloglu, G. Aydin, and U. R. Acharya, "Automated detection of diabetic subject using pre-trained 2d-cnn models with frequency spectrum images extracted from heart rate signals," *Computers in biology and medicine*, vol. 113, p. 103387, 2019.
- [21] T. Saba, A. S. Mohamed, M. El-Affendi, J. Amin, and M. Sharif, "Brain tumor detection using fusion of hand crafted and deep learning features," *Cognitive Systems Research*, vol. 59, pp. 221–230, 2020.
- [22] U.-O. Dorj, K.-K. Lee, J.-Y. Choi, and M. Lee, "The skin cancer classification using deep convolutional neural network," *Multimedia Tools and Applications*, vol. 77, no. 8, pp. 9909–9924, 2018.
- [23] S. H. Kassani and P. H. Kassani, "A comparative study of deep learning architectures on melanoma detection," *Tissue and Cell*, vol. 58, pp. 76–83, 2019.
- [24] D. Ribli, A. Horv'ath, Z. Unger, P. Pollner, and I. Csabai, "Detecting and classifying lesions in mammograms with deep learning," *Scientific reports*, vol. 8, no. 1, pp. 1–7, 2018.
- [25] N. A. El-Hag, W. El-Shafie, G. M. El-Banby, E.-S. M. El-Rabaie, A. S. El-Fishawy, A. El-Samie, and I. Fathi, "An efficient framework for macula exudates detection in fundus eye medical images," *Menoufia Journal of Electronic Engineering Research*, vol. 29, no. 1, pp. 78–83, 2020.
- [26] H. Khalil, N. El-Hag, A. Sedik, W. El-Shafie, A. E.-N. Mohamed, A. A. Khalaf, G. M. El-Banby, A. El-Samie, I. Fathi, and A. S. El-Fishawy, "Classification of diabetic retinopathy types based on convolution neural network (cnn)," *Menoufia Journal of Electronic Engineering Research*, vol. 28, no. ICEEM2019-Special Issue, pp. 126–153, 2019.
- [27] P. Kim, "Matlab deep learning," *With Machine Learning, Neural Networks and Artificial Intelligence*, vol. 130, p. 21, 2017.